Journal of Materials Chemistry C

Accepted Manuscript

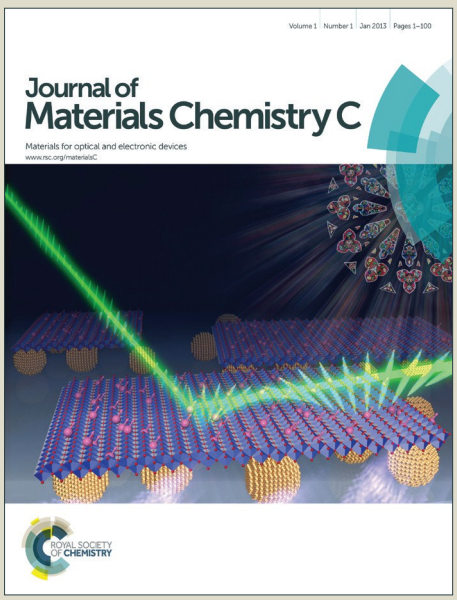

ROYAL SOCIETY OF CHEMISTRY

www.rsc.org/materialsC

Synthesis and Electrochromic, Halochromic and Electro-optical Properties of Polyazomethines with Carbazole Core and Triarylamine Units Serving as Functional Groups

Xiaochuan Ma[a], Haijun Niu[a]*, Hailin Wen[a], Shuhong Wang[a], Yongfu Lian[a], Xiankai Jiang[a], Cheng Wang[a], Xuduo Bai[a], Wen Wang[b]*

Abstract

A series of aromatic polyazomethines (PAMs) were prepared via the direct polycondensation from 9-(2-ethylhexyl)-carbazole-3, 6-dicarboxaldehyde and six different kinds of diamine containing triarylamines. The PAMs displayed good solubility in many organic solvents such as tetrahydrofuran (THF), chloroform ($CHCl_3$), N,N-dimethylformamide (DMF), et al which was beneficial for polymer film formation via spin coating, and exhibited outstanding thermal stability. These PAMs exhibited blue-green photoluminescence around 405-520 nm with quantum yield up to 48 % in dichloromethane (CH_2Cl_2) solution. They exhibited halochromic properties with color changing from yellow to red, and accompanied by fluorescence quenching after HCl-doped. The highest occupied molecular orbital (HOMO) and lowest unoccupied molecular orbital (LUMO) energy levels of these PAMs were determined from cyclic voltammograms as -5.01 to -4.88 eV and -2.15 to -2.11 eV, respectively. The PAMs films not only had good electrochromic properties with high coloration efficiency, but also generated photovoltagic and photocurrent under simulated solar radiation.

1. Introduction

Conjugated polymers (CPs) have been extensively studied for the different applications such as solar cells (SCs),[1-4] electrophotography,[5-7] organic field-effect transistors (OFETs),[8,9] organic

light-emitting diodes (OLEDs),[10-12] and nonlinear optical materials (NLO).[13] Recently, more and more attention has been paid to electrochromic properties of CPs (such as polyaniline (PANI), polythiophene (PTh), polypyrrole (PPy)).[14-16] Reynolds synthesized systematically and intensively studied thiophene derivatives which have excellent electrochromic properties.[17-19]

PAMs with aromatic backbones are attractive CPs with high performance and a particular series of electrochromic materials due to the nitrogen atom in the main chain with hybridization sp^2. They are similar to poly(p-phenylenevinylene)s (PPV) since the C=N group is isoelectronic with the C=C group. And PAMs are particularly interesting as CPs due to their documented excellent thermal, mechanical, electronic, optical, optoelectronic, and fiber forming properties.[20,21] Introducing -N=C- into the backbone of polymer is a facile alternative to coupling method for the preparation of conjugated compounds. Iwan has investigated systematically PAMs for photovoltaic applications in SCs,[22] and the power conversion efficiency (PCE) obtained by their groups has improved enormously to 0.56%.[23] Our groups studied hole transportation of PAMs in OLED and electrochromic properties of PAMs in electrochromic devices.[24,25]

Carbazole (CZ) and its derivatives are also investigated due to well-known hole transportation, photoluminescence, inherent electron donating nature and excellent photo conductivity. CZ has become one of the most common building blocks, particularly in design of compounds where intramolecular/intermolecular charge transfer happens.[26-29] The substituents in the 3rd and 6th positions of 9-carbazolyl can modulate hole-transporting properties, triplet energy levels.[30] Eyup Ozdemir prepared a coupled pyrrole-carbazole-pyrrole polyimine and studied electro–optical properties and electrochromism;[31] Mircea Grigoras synthesized and characterized some carbazole-based polyimines too.[32]

Highly electron-rich and redox-active compounds are useful building blocks in optic-electronic materials. Triarylamines (TA) is a unique molecule possessing particular functions such as its outstanding redox activity,[33] fluorescence, liquid crystalline properties, high oxidizability of the nitrogen atom.[34] For this reason, the polymers bearing TA structure have been investigated as transportability of positive charge centers via the radical cation species. The PAMs containing TA and a lone pair of nitrogenatom in the imine group (C=N) backbone can form intra- or inter-molecular interactions such as hydrogen bonding with other groups[35]. Furthermore, they also have the capabilities of protonation and complexation with metal ions, acid and iodine. A series of high-performance PAMs have been investigated extensively, with attractive electrochromic properties bearing TA derivatives. Hindson analyzed photovoltaic properties of TA-based PAMs.[36] Chen investigated donor-acceptor systems containing TA blocks deeply.[37]

The common CPs are difficult to be dissolved and melted. Over the past 25 years, different methods have been adopted toward processable PAMs by introducing various substituted groups (thiophene, phenylquinoxaline ring) and bulk monomers containing certain heterocyclic units (cardo-structure, tetraphenylethene) in the main chain.[38] Among them, the introduction of bulky TA into PAMs is an effective approach to reduce their trend of aggregation and to decrease the crystallization propensity with the aim to increase the solubility of the polymers.[39]

This paper presents the preparation of PAMs which not only combine the electron-donating properties of CZ and TA, but also utilize the electrochromic properties of CZ and TA. The purpose of this work is to demonstrate photophysics, halochromism, and electrochromism of six kinds of new TA-based PAMs with different substituted groups stimulated by irradiation, acid and electrooxidation.

2. Experimental

2.1 Materials

N,N-di(1-naphthyl)-4,4′-benzidine, N,N′-di-2-naphthalenyl-1,4-benzenediamine were bought from Qinhuangdao Bright Chemical Co. LTD; p-toluidine, 4-ethoxyaniline N,N′-diphenyl benzidine N,N′-diphenyl-1,4-phenylenediamine were purchased from TCI Co.; 9-(2-ethylhexyl)-carbazole- 3,6-dicarbox aldehyde was bought from Aldrich–Sigma Co.; Pd/C (10%) was purchased from Acros; THF, dimethylacetamide (DMAc), dimethylsulfoxide (DMSO), DMF, xylene, were supplied from Sinopharm Chemical Reagent Co. LTd; Lithium perchlorate ($LiClO_4$) was dried under vacuum at 120 ^oC for 36 h. 4,4′-bisamine-4″-ethyoxyl triphenylamine (1), 4,4′-bisamine-4″-methyl triphenylamine (2), N,N′-bis(4-aminophenyl)-N,N′-di-1-naphthalenyl- [1,1′-biphenhyl]-4,4′-diamine (3), N,N′-bis(4-aminophenyl)-N,N′-diphenyl-4,4′-biphenyldiamine (4), N,N′-bis(4-aminophenyl)-N,N′-di-2-naphthalenyl-1,4-benzene diamine (5) and N,N-bis(4-aminophenyl)-N′,N′-diphenyl-1,4-phenylene diamine (6) were prepared by Ullman reaction according to the method described in the literature.[40,41]

2.2 Synthesis of polymers

The synthesis of PAM1 was used as an example to illustrate the general synthetic procedure. To a three necked 50 ml glass reactor fitted with a magnetic stirrer, Dean-Stark trap and reflux condenser, 0.1559 g (0.47×10^{-3} mol) 4,4′-bisamine-4″-ethyoxyl triphenylamine was dissolved in DMSO following by adding 0.1568 g (0.47×10^{-3} mol) 9-(2-ethylhexyl)-carbazole-3,6-dicarboxaldehyde under nitrogen. Then, the mixture solution of dialdehyde and diamine (1:1

mol/mol) in 10 ml DMSO and 2 ml xylene was stirred at 160 ^{o}C for 20h. After the reaction, the obtained polymer solution was poured slowly into 400 ml of ice frozen water. The precipitate was collected by filtration, washed thoroughly with hot methanol in a Soxhlet apparatus for 48 h, then was dried under vacuum at 70 ^{o}C overnight. Yield: 0.2264 g, 76.7%, bright yellow. FTIR (KBr, cm^{-1}): 2956, 2922, 2853 (methyl and ethyl C-H stretching), 1619 (CH=N), 1593, 1492 (aromatic ring of benzene), 1312, 1264 (C-N), 1193 (C-C), 833 (p-substituted benzene), 695 (single substituted benzene). Anal. Calcd for PAM1 ($C_{42}H_{42}N_4O$, 618.37): C, 81.52%; H, 6.84%; N, 9.05%. Found: C, 81.46%; H, 6.60%; N, 8.19%.

^{1}H NMR (400 MHz, $CDCl_3$, ppm): 8.71 (s, -CH=N-), 8.00-8.10 (m, aromatic ring of benzene -CH=N-), 7.51-6.90 (m, aromatic ring of triphenylamine), 3.69-4.28 (m, -O-C-H), 0.86-2.23 (m, methyl and ethyl -C-H). ^{13}C NMR (100 MHz, $CDCl_3$, δ, ppm) 159.1 (-CH=N-).

The other polymers were prepared by an analogous procedure shown as Scheme 1.

Synthesis of PAM2. Yield: 0.2021 g, 77.0%, yellow. FTIR (KBr, cm^{-1}): 3027, 2931, 2847 (methyl and ethyl C-H stretching), 1616 (CH=N), 1595, 1525, (aromatic ring of benzene), 1315, 1262 (C-N), 1185, 1127 (C-C), 810 (p-substituted benzene), 722 (single substituted benzene). Anal. Calcd for PAM2 ($C_{41}H_{40}N_4$, 588.37): C, 83.64%; H, 6.85%; N, 9.52%. Found: C, 83.09%; H, 6.80%; N, 8.59%. ^{1}H NMR (400 MHz, $CDCl_3$, ppm): 8.70 (s, -CH=N-), 8.02-8.22 (m, aromatic ring of benzene -CH=N-), 7.49-7.12 (m, aromatic ring of triphenylamine), 4.25-4.27 (m, -CH-), 0.86-2.64 (m, methyl and ethyl -C-H). ^{13}C NMR (100 MHz, $CDCl_3$, δ, ppm) 158.6 (-CH=N-).

Synthesis of PAM3. Yield: 0.3225 g, 83.2%, yellow. FTIR (KBr, cm^{-1}): 3021, 2920, 2853 (methyl and ethyl C-H stretching), 1618 (CH=N), 1568, 1492 (aromatic ring of benzene), 1314, 1269

(C-N), 1181, 1123 (C-C), 814 (p-substituted benzene), 692 (single substituted benzene). Anal. Calcd for PAM3 ($C_{66}H_{55}N_5$, 916.98): C, 86.33%; H, 6.04%; N, 7.63%. Found: C, 85.09%; H, 6.00%; N, 7.40%. ^{1}H NMR (400 MHz, $CDCl_3$, ppm): 8.71 (s, -CH=N-), 7.82-8.12 (m, aromatic ring of benzene -CH=N-), 7.49-7.02 (m, aromatic ring of triphenylamine), 4.26-4.29, (m –CH-), 0.86-2.83 (m, methyl and ethyl -C-H). ^{13}C NMR (100 MHz, $CDCl_3$, δ, ppm) 158.7 (-CH=N-).

Synthesis of PAM4. Yield: 0.2672 g, 71.6%, bright green yellow. FTIR (KBr, cm^{-1}): 2924, 2856 (methyl and ethyl C-H stretching), 1618 (CH=N), 1589, 1488 (aromatic ring of benzene), 1312, 1271 (C-N), 1181, 1126 (C-C), 815 (p-substituted benzene), 697 (single substituted benzene). Anal. Calcd for PAM4 ($C_{58}H_{51}N_5$, 816.86): C, 85.16%; H, 6.28%; N, 8.56%. Found: C, 84.67%; H, 6.24; N, 7.95%. ^{1}H NMR (400 MHz, $CDCl_3$, ppm): 8.70 (s, -CH=N-), 8.05-8.12 (m, aromatic ring of benzene -CH=N-), 7.51-7.08 (m, aromatic ring of triphenylamine), 4.24-4.27, (m –CH-), 0.87-2.60 (m, methyl and ethyl -C-H). ^{13}C NMR (100 MHz, $CDCl_3$, δ, ppm) 159.1 (-CH=N-).

Synthesis of PAM5. Yield: 0.2129 g, 80.6%, bright yellow. FTIR (KBr, cm^{-1}): 3056, 2961, 2870 (methyl and ethyl C-H stretching), 1622 (CH=N), 1595, 1496 (aromatic ring of benzene), 1314, 1271 (C-N), 1183, 1119 (C-C), 813 (p-substituted benzene), 693 (single substituted benzene). Anal. Calcd for PAM5 ($C_{60}H_{51}N_5$, 838.89): C, 85.58%; H, 6.10%; N, 8.32%. Found: C, 85.57%; H, 5.37%; 8.20. ^{1}H NMR (400 MHz, $CDCl_3$, ppm): 8.68 (s, -CH=N-), 7.82-8.12 (m, aromatic ring of benzene -CH=N-), 7.53-7.12 (m, aromatic ring of triphenylamine), 4.20-4.26 (m –CH-), 0.86-3.03 (m, methyl and ethyl -C-H). ^{13}C NMR (100 MHz, $CDCl_3$, δ, ppm) 159.5 (-CH=N-).

Synthesis of PAM6. Yield: 0.3005 g, 81.5%, green yellow. FTIR (KBr, cm^{-1}): 3034, 2936, 2855 (methyl and ethyl C-H stretching), 1619 (CH=N), 1593, 1494 (aromatic ring of benzene), 1313,

1269 (C-N), 1193, 1128 (C-C), 830 (p-substituted benzene), 694 (single substituted benzene). Anal. Calcd for PAM6 ($C_{52}H_{47}N_5$, 738.77): C, 84.18%; H, 6.38%; N, 9.44%. Found: C, 84.05%; H, 6.75%; N, 8.47% ^{1}H NMR (400 MHz, $CDCl_3$, ppm): 8.70 (s, -CH=N-), 7.92-8.22 (m, aromatic ring of benzene -CH=N-), 7.55-7.02 (m, aromatic ring of triphenylamine), 4.20-4.30, (m –CH-), 0.86-2.33 (m, methyl and ethyl -C-H). ^{13}C NMR (100 MHz, $CDCl_3$, δ, ppm) 159.1 (-CH=N-).

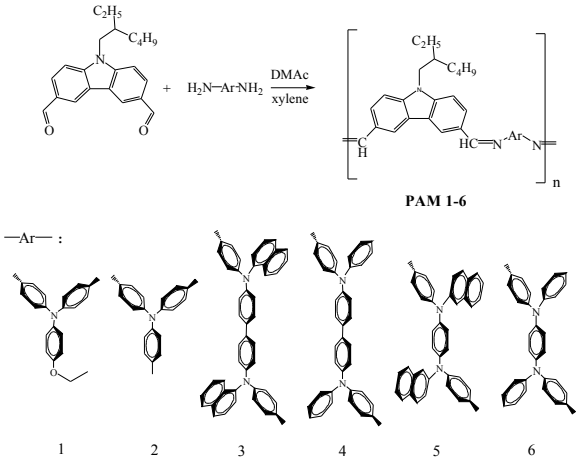

Scheme.1. Synthetic routes for PAM 1-6 with different diamines.

2.3 Measurements

The obtained PAMs were characterized by the following techniques: FT-IR spectra were recorded on a PerkinElmer Spectrum 100 Model FT-IR spectrometer. ^{1}H NMR spectra were measured on a Bruker AC-400 MHz spectrometer in $CDCl_3$, using tetramethylsilane as an internal reference. UV–vis spectra were determined on a UV-3600 (Shimadzu). Thermogravimetric analysis (TGA) was conducted with approximately 6–8 mg powder samples heated in flowing nitrogen (flow rate = 10 cm^3/min) at a heating rate of 10 ^oC/min using a conducted with a PerkinElmer Pyris 6 TGA. Gel permeation chromatography (GPC) analysis was performed on a Malvern instrument connected with one refractive index detector (Viscotek-VE3580-RI- DETECTOR) by using a polymer/THF solution at a

flow rate of 1.0 ml/min at 35 ^{o}C and calibrated with polystyrene standards. Cyclic voltammetry (CV) measurements were conducted on a CH Instruments 660 A electrochemical analyzer at a scan rate of 50 mV/s in 0.1 mol/L $LiClO_4/CH_3CN$. For the electrochromic investigation, PAMs films were spun coating on an ITO-coated glass slide and a homemade electrochemical cell was built from a commercial UV-vis cuvette. The cell was placed in the optical path of light beam in a UV-vis spectrophotometer, which allowed acquiring electronic absorption spectra under potential control in a 0.1 mol/L solution of $LiClO_4$ as an electrolyte under nitrogen atmosphere in dry CH_3CN. The thicknesses of PAMs films were determined on profile-system XP-100 (KLA-Tencor) by comparing to the thickness of blank ITO-coated glass. The oxidation and reduction potentials of polymer films were measured using a Pt wire and an Ag/AgCl electrode as a counter electrode and a quasi-reference electrode respectively, and calibrated against the ferrocene/ferrocenium (Fc/Fc^+) redox couple by assuming the absolute energy level of Fc/Fc^+ as -4.80 eV to vacuum. Photocurrent response of PAMs was determined upon irradiation on and off with a 500W Xe arc lamp supported by Beijing ChangTuo Co. Density-functional theory (DFT) calculations were performed on a computer. Geometry optimizations were carried out using the B3LYP functional as implemented in Gaussian 98 program. The highest-occupied molecular orbital (HOMO) and lowest-unoccupied molecular orbital (LUMO) energy levels of the polymers were calculated by the onsets of oxidation potentials of the polymer films.[42]

3. Results and discussion

3.1 Synthesis and characterization of polymers

The PAMs were prepared from 9-(2-ethylhexyl)-carbazole-3, 6-dicarboxaldehyde and diamines containing TA unit. The process was accomplished through a facile one-step polycondensation under N_2 atmosphere condition without any catalysts. The structures of polymers were confirmed by FT-IR spectroscopy which showed a strong absorption band at 1618 cm^{-1}, assigned to the azomethine (C=N) stretching. The introduction of alkyl group increased solubility of the PAMs which were dissolved well in common organic solvents, such as $CHCl_3$, DMSO, NMP, DMAc, DMF, and THF. Azomethine formation was unequivocally proven by the characteristic imine protons at 8.70 ppm in ^1H NMR and 159 ppm in ^{13}C NMR spectra (Fig. S1).

3.2 Thermal properties and molecular weight

Fig.1 depicts a typical set of TGA curves for PAMs in nitrogen, and the results are summarized in Table 1. All the PAMs exhibited good thermal stability with a 10 wt% loss at temperature of above 390 ^oC. Through the table, PAM1 revealed the lowest 5 wt% at 300 ^oC due to the instability of ethyoxyl groups. The 20% weight loss temperatures of these PAMs in nitrogen were recorded in the range of 465-530 ^oC. The amount of carbonized residue (char yield) of these polymers in a nitrogen atmosphere was more than 45% (PAM6) at 700 ^oC. The high char yields of PAMs could be ascribed to their high aromatic content.

Fig. 1

Fig.1. TGA curves of PAM1 to PAM6.

For smart glass, the original color of PAMs at neutral form should be light-yellow or colorless in contrast with doped form which should be deep color to be distinguished in anodic

electrochromic materials. The molecular weight of PAMs was measured by GPC, using polystyrenes standards and THF as eluent. The weight-average molecular weight ($\bar{M}_w$) and polydispersity (PDI) were determined as 6100–88300 g/mol and 1.39–1.57, respectively (Table 1). In general, the effective high degree of conjugation makes the high molecular weight polymer insoluble which is responsible for $\bar{M}_w$s of PAMs containing naphthalenyl lower than the others. The calculated GPC data confirm that DP_n of PAM3 (12) was smaller than PAM4 (23).

Table 1

Table 1 Thermal properties and molecular weights of the PAMs

	5%	10%	20%	Char yield[a] wt%	M_w[b](g/mol)	M_n[b](g/mol)	PDI[c]	DP_n[d]
PAM1	300	390	465	53	13700	10000	1.37	16
PAM2	455	470	490	61	6100	4400	1.39	7
PAM3	460	490	520	59	15600	10800	1.44	12
PAM4	470	495	530	71	34400	19100	1.80	23
PAM5	450	480	510	55	16200	10000	1.62	12
PAM6	380	460	490	45	88300	56400	1.57	76

[a] Residual weight percentage at 700 ^oC in nitrogen.

[b] Calibrated with polystyrene standards, using THF as the eluent at a constant flow rate of 0.8 mL/min at 35 ^oC.

[c] Polydispersity index (M_w/M_n).

[d] Average number degree of polymerization.

3.3 Optical properties

The UV-visible absorption spectra of PAMs in CH_2Cl_2 are shown in Fig.2 (A). From the figure, all the UV absorption peaks of PAMs exhibited strong absorption at 330–390 nm, assigned to the π–π* transition resulting from the conjugation between the aromatic

rings and TA units combined by C=N double bonds in the PAMs backbone. In the solid state, the maxima absorption spectra of PAMs were centered at 340-400nm (Table 2). The solid films of PAM3 (400nm) and PAM4 (350nm) were found to be bathochromically shifted (15nm and 5nm) from the corresponding dilute solution. In fact, the dihedral angles between the mean planes described by the central CZ and the C=N group for PAM3 and PAM4 are 20^{o} and 17^{o} (Fig S2) respectively. This is smaller than the angle of other PAMs between C=N group and CZ unit. The data confirms that of PAM3 and PAM4 with biphenyl group are co-planar with slight twisting between the C=N bond and CZ unit. The lower E_gs and higher degree of conjugations of PAM3 and PAM4 relative to the other polymers are most likely responsible for the bathochromic shift observed for the films relative to the corresponding solution. But, PAM1, PAM2, PAM5 and PAM6 revealed the similar maximum absorption in solid state compared to that in the solution. The bigger dihedral angles of molecular chain resulted in disturbing the effective aggregation.

Fig. 2

Fig.2. UV-visible absorption spectra (A) and PL spectra (B) of PAMs in CH_2Cl_2 at room temperature, (C) the CIE 1931 (x, y) chromaticity diagram of PAMs.

As shown in Fig.2 (B), the PL spectra of PAMs were measured in CH_2Cl_2 (conc: 10^{-6}mol/L). For PAMs, the emission color range from blue (PAM6, CIE 1931: x, 0.1535; y, 0.1109) to green-blue (PAM5, CIE 1931: x, 0.3235; y, 0.4389). Furthermore, PAM5 and PAM6 exhibited green-blue and green PL emission, respectively.

The φs of these PAMs after refractive index correction[43] were calculated and summarized in Table 2. The PAMs exhibited PL emission maxima around 405-530 nm in

CH_2Cl_2 solution with PL quantum yield from 4 to 48%. The PL intensities decreased in the order: PAM4 > PAM2 > PAM5 > PAM6 > PAM3 > PAM1, almost corresponding to the energy gap (PAM4 > PAM3> PAM5 > PAM6 > PAM2 >PAM1). The fluorescence of PAM2 is less than PAM3 most likely from nonradiative internal conversion involving vibrational energy dissipation either by bond rotation or with the solvent.[44]

Table 2

Table 2 Optical and electrochemical properties for PAMs.

	$\lambda_{solution}^{abs}$ (nm)[a]	$\lambda_{solution}^{PL}$ (nm)[a]	λ_{film}^{abs} (nm)[b]	λ_{onset}^{abs} (nm)[b]	Φ^{c} (CH_2Cl_2)%	$E_{1/2}$ vs Ag/AgCl[d]	E_{onset}^{peak} vs Ag/AgCl	$E_{HOMO}^{electro}$ (eV)[f]	$E_{LUMO}^{electro}$ (eV)[f]	E_g^{film} (eV)[e]	E_{HOMO}^{quntum} (eV)[g]	E_{LUMO}^{quntum} (eV)[g]	E_g^{quntum} (eV)[g]
PAM1	340	405	340	435	4	0.77	0.66	-5.01	-2.15	2.86	-4.46	-1.53	2.93
PAM2	350	405	350	450	22	0.88	0.65	-5.00	-2.24	2.77	-4.48	-1.59	2.89
PAM3	385	505	400	445	5	0.98	0.80	-5.15	-2.36	2.79	-4.36	-2.07	2.29
PAM4	345	480	350	435	48	0.87	0.67	-5.02	-2.17	2.85	-4.51	-2.29	2.22
PAM5	340	530	340	445	11	0.74	0.55	-4.90	-2.11	2.79	-4.30	-1.61	2.69
PAM6	340	405	340	450	10	0.72	0.53	-4.88	-2.11	2.77	-4.43	-1.58	2.85

[a] UV–vis absorption and PL spectra measurements in CH_2Cl_2 at room temperature.

[b] λ_{onset} of the polymer film.

[c] The quantum yield was calculated with quinine sulfate as the standard (ϕ = 54.6%).

[d] $E_{1/2}$: average potential of the redox couple peaks.

[e] $E= 1240/\lambda_{onset}$.

[f] The HOMO energy levels were calculated from cyclic voltammetry and were referenced to ferrocene (4.8 eV). $E_{LUMO} = E_{HOMO} + E_g$, $E_{ox/onset}$ *(Fc/Fc vs Ag/AgCl)* = 0.45 V, E_{HOMO}=*-e(E_{OX}+4.35)eV*.

[g] Quantum theoretical calculation of the PAMs.

3.4 Halochromic properties

As shown in the spectra (Fig.3), initially neutral PAM3 and PAM6 solution reveal the absorption λ_{max} at 390 and 335, 400 nm, respectively. The absorbance of PAM3 and PAM6 was bathochromically shifted by 120 and 110 nm, respectively, when exposed to HCl vapor. These polymers showed new absorbances at 335, 505 and 510 nm with HCl

exposure. Their apparent color turned from yellow to red upon acid vapor exposure. Similar changes were seen with the other PAMs in Fig.S3. As showed in Fig.S4, PAM6 reveal the switching time of 3.6 s and the bleaching time of 4.6 s. At the end of the process, the solution returned to its original yellow color when exposed to NH_3 vapor. Upon doping with HCl, the electron pair on nitrogen, generating a positive charge on the nitrogen atom was stabilized by a chloride anion.[45]

Fig. 3

Fig.3. Absorbance spectral changes of PAM3 and PAM6 in CH_2Cl_2 when protonated with HCl vapor in steps during the same time interval. The concentration of pure PAMs was 0.034 mg/L. Inset: photographs showing the color changes upon HCl vapor exposure. The undoped molecular structure and protonated extreme resonance forms of PAMs shown on right.

Nitrogen atom in the imine linkage (C=N) doped by acid created a positive charge that mostly caused an intramolecular change transfer, causing the color change. The protonation of the C=N in PAMs also resulted in a much stronger electron-accepting center, which enhances the charge separation of π-electrons in the conjugated polymer with donor-acceptor structure. Therefore these effects enhance electron cloud overlap and reduce the band gap, then the color of the solution containing PAMs can changed with pH values. From the UV-vis spectra, it can be found that the spectra of PAMs doped by HCl restored easily when undoped by NH_3. And the consistent isosbestic points observed with repeated protonation/unprotonation provide additional evidence for the stability of the protonated intermediate. It additionally confirms that the neutral form is reversibly converted to the protonated form without decomposition, which was similar to the reported phenomena.[46] The bands of PAM3 were almost same to that of PAM6 with color changing

to red gradually. Particularly, the concentration of HCl vapor was very dilute, which implied PAMs were especially sensitive to pH value.

Fig. 4

Fig.4. Photograph of the PL of PAM3 and PAM6 in the silica gel plate upon UV exposure (excited at 365 nm).

On the other hand, the photoluminescence of PAMs gradually disappeared when exposed to HCl vapor. With the continuous exposure to HCl vapor, the photoluminescence of PAMs were quenched gradually (Fig. 4), but it restored after NH_3 doping. In most of the cases azomethine protonation was suggested to increase fluorescence with rotational deactivation and photoisomerization. But, this time the PAMs protonated by HCl would form hydrogen bonding to the nitrogen of C=N, and such hydrogen bonding would enhance charge separation. As a result, increasing strength of intramolecular charge transfer decreased the fluorescence efficiency, which was consistent with the observation by Jenekhe.[47] Combining with the fluorescence quenching mechanism proposed by Skene, photoinduced electron transfer might occur to deactivate the singlet excited state.

3.5 Electrochemical properties

The electrochemical properties of these PAMs were investigated by CV with the cast film on an ITO-coated glass substrate as working electrode, and the whole test procedures were tested under nitrogen atmosphere. The thicknesses of the PAMs were measured as about 1μm. For comparison, one pair of reversible redox peaks for dialdehyde were determined at 1.7 V in the CV scans of monomers (Fig.S5). This implied that the lone pair of electrons on the nitrogen atom of CZ group was localized within the coplanar ring and encouraged the CZ group to be a weaker electrondonor.

Compared to the electrochemical data curves of PAMs (Fig.5), the oxidation of dialdehyde was more difficult. As a bridge linked triphenylamine (TPA) and CZ unit, the -CH=N- blocks were not oxidized, and the attracting electron effect of the C=N bond increased in the oxidation potential of the compound. Thus, the reduction-oxidation reactions of PAMs occurred at the TPA unit in the diamine component.

Fig. 5

Fig.5. Cyclic voltammetry for PAMs in CH_3CN containing 0.1mol/L $LiClO_4$, at a scan rate of 50 mV/s.

The cyclic voltammograms of PAM1 to PAM4 pointed out oxidative peaks at 0.93, 0.95, 1.0 and 0.79 V respectively, and the corresponding reductive peaks at 0.61, 0.81, 0.91 and 0.96 V respectively. On the contrary, PAM5 and PAM6 exhibited similar couple of symmetrical redox waves, in which the oxidative peaks at 0.79 and 1.1 V (PAM5) 0.77 and 0.98 V (PAM6), respectively; the reductive peaks at 0.68, 0.98 (PAM5), and 0.67, 1.1 V(PAM6), respectively. A linear dependence of the peak currents as a function of scan rates confirmed both a nondiffusional redox process and a well-adhered electroactive polymer film (Fig. S6). Because of the stability of the films and good adhesion between the polymer and ITO substrate, PAM3 and PAM5 exhibited excellent redox stability. When compared with the cyclic voltammetry, two oxidation processes occurred for PAM5, whereas both PAM2 and PAM3 had only one oxidation process observed by differential pulse voltammogram (DPV) which is shown in Fig (S7).[48] The simplified redox process of PAM2 could be proposed from its neutral state to radical cation state, in which nitrogen atom of TPA is the redox reaction center corresponding to the site of electrochemical reactions. Moreover, the anodic processes of PAM3 and PAM5 were investigated with

equimolar ferrocene, a linear dependence of the currents as a function of the square root (Fig S8). The number of electrons involved in the oxidation process was derived by comparing the intensity of the anodic current of ferrocene under such conditions. According to the simplified Randles−Sevcik equation, the number of electrons involved in the oxidation was calculated by comparing the peak currents of ferrocene to the given sample for the scans rates.[49] This can be suggested that the oxidation processes of PAM3 and PAM5 were both one single oxidation involving two electrons. As for PAM3 having two amino centers in one repeat unit (containing two TPA in one repeat unit), the first and second oxidations happened simultaneously while electrons were lost from the two definitely separated TPA units resulting in a two separated radical cations on account of the block of biphenyl-linkage between two amino centers. In other words, there is not stable single radical cation in this case, so two amino centers in one unuit would be oxidized at the same time with a color changing from light-yellow (neutral state) to red (oxidized state). But for the PAM5, two oxidation stages should be attributed to successive two electrons removal from the repeat unit gradually. These oxidation processes of PAM5 are associated with monocation and dication formations of the two amino centers. Accompanied with two-electron oxidation, the color changed from yellow (neutral state) to red (first oxidized state), finally to blue (second oxidized state). According to the electronic transfer process suggested by Liou,[50] the proposed simplified redox process was proposed as Scheme 2.

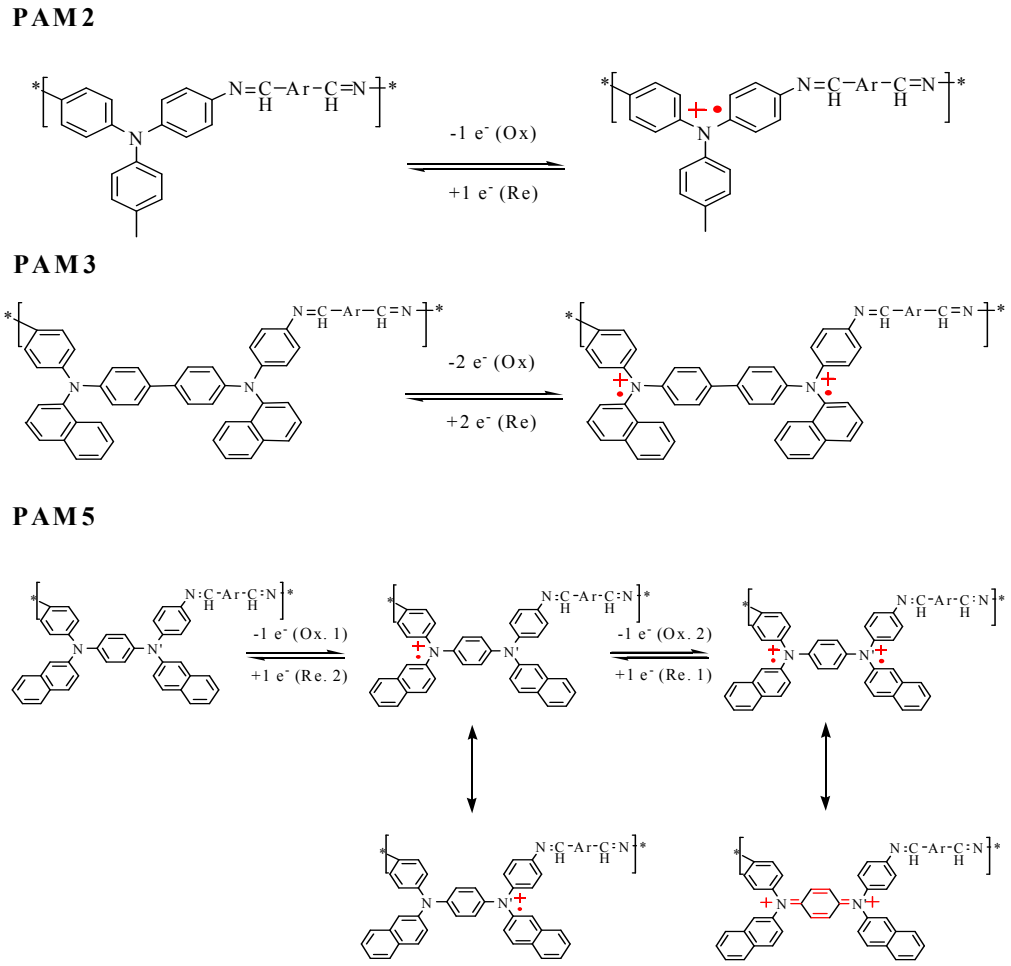

Scheme.2. Proposed simplified redox process and the resonance form of PAM2, PAM3 and PAM5.

3.6 Quantum chemistry calculation

To obtain the energy levels of the HOMO and the LUMO of the polymers, the ferrocene/ferrocenium (Fc/Fc^{+}) vs Ag/AgCl can be used to calculate the onset oxidation potentials (E_{onset}) or half-wave potentials ($E_{1/2}$) in the table 2, whose redox potential is assumed to have an absolute energy level of -4.80 eV compared to vacuum to obtain accurate redox potentials of electrode.

The HOMO energy values from PAM1 to PAM6 were calculated to be at in the range from −5.01 to −4.88 eV in Table 2. Generally, high HOMO energy level easily results in

electron escaping, and effective antioxidant property requires higher HOMO energy level than -5.27 eV (the air oxidation threshold, ca. -5.27 eV).[51] The HOMO energy levels of PAMs were in the order with PAM3 > PAM4 > PAM1 > PAM2 > PAM5 > PAM6.

It is indicated that PAM3 had the strongest antioxidation properties among the studied polymers due to the lowest experimental HOMO energy level. Because of the reduction curves could hardly be obtained, the LUMO energy levels of the PAMs were estimated from the E_{HOMO} and E_g. So the E_{LUMO}s were in the range from -2.15 (PAM1) to -2.11 eV (PAM6), respectively. To further understand the electronic structures of the polymers, and then to provide key parameters for the design of devices, it is necessary to determine HOMO and LUMO energy levels of the polymers.

Through the Fig.6, the actual data of E_g were in the order with PAM1 > PAM2 > PAM6 > PAM5 > PAM3 > PAM4, which has a slight deviation compared with the theoretical data. That was due to the interaction of the solvation process, molecular structure and the electron of the electron-withdrawing group.

The different site linked TA played the key role in the electron structure and regulated the gaps of PAMs. The suitable energy levels of the conjugated PAMs indicate the PAMs could be used as charge transportation materials in PLED and solar cell.

Fig. 6

Fig.6. Pictorial representations (a) of the electron density in the frontier molecular-orbitals of repetition units and pictorial energy gap (b) of PAMs.

3.7 Electrochromic properties

Fig. 7

Fig.7. Electronic absorption spectra of films of PAM2 (a) and PAM5 (b) and their 3D spectra

respectively, in the process of electrochemical doping with 0.1 V potential intervals in CH_3CN containing 0.1mol/L $LiClO_4$ as the supporting electrolyte (vs Ag/AgCl).

The PAM solution was cast onto an ITO-coated glass substrate, and their electrochromic absorption spectra were monitored with a UV–vis spectrometer at different applied potentials. The typical electrochromic absorption spectra of PAM2 and PAM5 are shown in Fig.7, and other electrochromic absorption spectra of PAMs are shown in Fig.S9. The absorption of PAM2 started to change at 410 nm in which characteristic of π –π* transition happened in TPA at 1.3 V, and the new peaks of the PAM2 did not appear at the beginning of doping. When the applied potentials increased positively from 1.3 to 2.3 V, the characteristic absorbance peak at 410 nm decreased gradually, and one new band grew at 520 nm with the color changed from yellow to red. For the peak of the PAM5, the film exhibited strong absorption at 405 nm at 0 V. When the applied potential of PAM5 was in the region from 0.6 to 1.2 V, new bands grew up at 540 and 1,040 nm in the NIR region gradually increased in intensity. While the absorption at 405 nm of PAM5 fade away, and the color changed from yellow to red.

3.8 Spectroelectrochemical properties

Fig. 8

Fig.8.(a) Potential step absorptometry (upper) and (b) current consumption (lower) of PAM5 at 505 nm (in 0.1 mol/L $LiClO_4$/CH_3CN as the supporting electrolyte) by applying a potential step (0.00-0.80 V) with a cycle time of 10 s.

The stability, response time, and coloration efficiency are the key parameters for an electroactive polymer film to be amenable for usage in optical and electrochromic devices, thus the electrochromic switching studies were further measured.

For optical switching studies in Fig.8 (a), the color switching times were estimated by applying a potential step, and the absorbance profiles were monitored. The switching time is defined as the time required for reach 90% of the full change in absorbance after the switching of the potential. The PAM5 film revealed switching time of 2.6 s at 0.80 V for coloring process at 505 nm and 2.4 s for bleaching. After continuous cyclic scans between 0.00 V and 0.80V in 300 s, the polymer films still exhibited excellent stability of electrochromic characteristics, indicating that the film was very stable and had good adhesion on the ITO substrate. The color switching time shown above was somewhat slower than the bleaching switching time of 0.2 s for electrochromic polymer films. This may be due to slow ion permeation in the film of PAMs.

The electrochromic coloration efficiency (CE: η) is also an important characteristic for the electrochromic materials. η can be calculated using the equations given below:

$$\Delta_{OD} = log\left({}^{T_b}/_{T_c}\right)$$

$$\eta = {}^{\Delta_{OD}}/_{Q}$$

where T_b and T_c are the transmittances before and after coloration, respectively, Δ_{OD} is the change of the optical density, which is proportional to the amount of created color centers. Q (mC/cm^2) denotes the amount of injected/ejected charge per unit sample area. Through the table 3 it can be concluded that the order of PAMs are PAM5 (246) > PAM4 (166) > PAM6 (83) > PAM2 (77) > PAM1 (73) > PAM3 (68). It showed that CE of PAM5 exhibits up to 246 cm^2/C at 505 nm and revealed highly stable electrochromic (the others were listed in Table 3), due to the same planarity between bond of C=N and benzene ring which are linked together with bond directly.

Table 3

Table. 3. Optical and electrochemical data collected for coloration efficiency measurements of PAMs.

Polymer code[a]	$\lambda_{(nm)}$[b]	δ_{OD}[c]	Q(mC/cm^2)[d]	η(cm^2/C)[e]
PAM1	505	0.0062	0.08	73
PAM2	500	0.0038	0.05	77
PAM3	510	0.022	0.32	68
PAM4	510	0.0066	0.04	166
PAM5	505	0.038	0.15	246
PAM6	525	0.052	0.70	83

[a] Switching between 0.0 and 0.8 V for PAMs (V vs Ag/AgCl).

[b] The given wavelength where the data were determined.

[c] Optical density change at the given wavelength.

[d] Injected charge, determined from the in situ experiments.

[e] Coloration efficiency is derived from the equation $\eta=\delta_{OD}/Q$.

3.9 Photoelectrical properties

Fig. 9

Fig.9. A typical photocurrent (lower) and photovoltaic (upper) response for an PAM6 film immobilized on ITO glass upon exposure to light with switching at room temperature. (b) photogenerated electrons flow scheme.

A reversible rise/decay of the photocurrent was observed when light switching on and off many times, as shown in Fig.9. For comparison the bare ITO did not exhibit the phenomena suggesting that the PAMs were responsible for photocurrent generation. A steady anodic photocurrent was obtained from the dye monolayer-modified electrode when

the PAMs/ITO electrode was illuminated under white light of 150 mW/cm^2 intensity without any bias voltage in 0.1mol/L $LiClO_4$ electrolyte solution.

Upon irradiation, the photocurrent (the anodic current polarity is negative) increased and rapidly reached an approximately steady-state value. The photocurrent returned to the low level after irradiation was terminated. Moreover, the current density decreased slightly after several on/off cycles. The photocurrent response of the PAMs films showed stably photoinduced. The photocurrent shown in Fig.9 also demonstrated the typical open-circuit photovoltaic response of electrode on illumination. After the light was turned off, the photovoltage decayed to the lowest slowly. On the contrast, after the light was turned on, the photovoltage increased instantly. A similar characteristic was observed for other PAMs of this series. Thus, these PAMs can act as the photoelectric conversion material for optoelectronic application. In the Fig.9 (b), under the push of illumination, the photo-generated electrons transported from the LUMO of the PAM6 (-2.11 eV) to the conduction band of the ITO surface (4.7 eV) and moved to the external circuit. Then the photocurrent generated among the particulate hopping of electrons. Through the figures, it is can be noted that the photocurrent and photovoltage decayed slightly after on/off illumination cycles procedure.

Conclusions

A series of highly stable anodic electrochromic polymers with excellent optical transmittance change have been synthesized from dialdehyde and different diamines. The PAMs displayed good solubility in many organic solvents such as THF, $CHCl_3$, DMF and DMAc which was beneficial for polymer film formation via spin coating. The polymers

exhibited excellent reversible electrochemical behavior and continuous cyclic stability of electrochromic characteristics. The color of PAMs could be varied from initial yellowish to red via electrooxidation. And multiple reversible colors states were also observed with pH doping. Thus, these PAMs can be used as new hole-transporting and electrochromic materials because of their proper E_{HOMO} values and stable electrochromic behavior, while the resulting polymers also exhibited potential applications in optoelectronics.

Acknowledgements

The authors are grateful to the support of the National Natural Science Foundation of China (Grant No.51373049, 51372055, 51303045, 51273056, 21372067), Doctoral Fund of Ministry of Education of China (20132301120004, 20132301110001).

References

[1] G.D. Sharma, S.G. Sandogaker, M.S. Roy, *Thin. Solid. Films,* 1996, 278, 129-134.

[2] S. Barik, T. Bletzacker, W.G. Skene, *Macromolecules,* 2012, 45, 1165-1173.

[3] A. Bolduc, S. Barik, M. R. Lenze, K. Meerholz, W.G. Skene, *J. Mater. Chem. A,* 2014, 2, 15620-15626.

[4] (a) B.C. Thompson, K.A. Abboud, J.R. Reynolds, K. Nakatani, P. Audebert, *New. J. Chem.,* 2005, 29, 1128-1134; (b) S. Beaupré, P-LT. Boudreault, M. Leclerc, *Adv. Mater.,* 2010, 22, 6-27.

[5] K-Y. Law, *Chem. Rev.,* 1993, 93, 449-486.

[6] S.L. Lin, L.H. Chan, R.H. Lee, M.Y. Yen., W.J. Kuo, C.T. Chen, R.J. Jeng, *Adv. Mater.,* 2008, 20, 3947-3952.

[7] Z.C. He, C. Zhang, X.F. Xu, L.J. Zhang, L. Huang, J.W. Chen, H.B. Wu, Y. Cao, *Adv. Mater.,* 2010, 23, 3086-3089.

[8] F. Otón, R. Pfattner, N.S. Oxtoby, T.M. Mas, K. Wurst, X. Fontrodona, Y. Olivier, J. Cornil, J. Veciana, C. Rovira, *J. Org. Chem.,* 2011, 76, 154-163.

[9] R.K. Cheedarala, G-H. Kim, S. Cho, J. Lee, J. Kim, H-K. Song, J.Y. Kim, C. Yang, *J. Mater. Chem.,* 2011, 21, 843-850.

[10] C. Adachi, K. Nagai, N. Tamot, *Appl. Phys. Lett.,* 1995, 66, 2679-2681.

[11] A.V. Dijken, J.J.A.M. Bastiaansen, N.M.M. Kiggen, B.M.W. Langeveld, C. Rothe, A. Monkman, I. Bach, P. Stossel, K. Brunner, *J. Am. Chem. Soc.,* 2004, 126, 7718-7727.

[12] P.T. Boudreault, S. Beaupré, M. Leclerc, *Polym. Chem.,* 2010, 1, 127-136.

[13] J. Kulhánek, F. Bureš, T. Mikysek, J. Ludvík, O. Pytela, *Dyes. Pigments.,* 2011, 90, 48-55.

[14] M. El-Khouly, Y. Chen, X.D. zhuang, S. Fukuzumi, *J. Am. Chem. Soc.,* 2009, 131, 6370-6371.

[15] A. Mishra, C-Q. Ma, P. Bauerle, *Chem. Rev.,* 2009, 109, 1141-1276.

[16] Gomez R, Blanco R, Veldman D, Segura JL, RAJ. Janssen, *J. Phys. Chem. B,* 2008, 112, 4953–4960.

[17] D.M. Welsh, A. Kumar, E.W. Meijer, J.R. Reynolds, *Adv. Mater.,* 1999, 11, 1379-1382.

[18] S. Alkan, C.A. Cutler, J.R. Reynolds, *Adv. Funct. Mater.,* 2003, 13, 331-336.

[19] C.R.G. Grenier, W. Pisula, T. Joncheray, K. Mullen, J.R. Reynolds, *Angew. Chem. Int. Ed.,* 2007, 46, 714-717.

[20] (a) C.J. Yang, S.A. Jenekhe, *Chem. Mater.,* 1991, 3, 878-887; (b) J.E. Kuder, H.W. Gibson, D. Wychick, *J. Org. Chem.,* 1975, 40, 875-879.

[21] G.S. Liou, H.Y. Lin, Y.L. Hsieh, Y.L. Yang, *J. Polym. Sci., Part A: Polym. Chem.,* 2007, 45, 4921-4932.

[22] (a) A. Iwan, M. Palewicz, A. Chuchmała, L. Gorecki, A. Sikora, B. Mazurek, G. Pasciak, *Synt. Met.,* 2012, 162, 143-153; (b) A. Iwan, E. Schab-Balcerzak, D. Pociecha, M. Krompiec, M. Grucela, P. Bilski, M. Kłosowski, H. Janeczek, *Opt. Mater.,* 2011, 34, 61–74; (c) A. Iwan, E. Schab-Balcerzak, K. P. Korona, S. Grankowska, M. Kamińska, *Synth. Met.,* 2013, 185-186, 17-24.

[23] A. Iwan, B. Boharewicz, K. Parafiniuk, I. Tazbir, L. Gorecki, A. Sikora, M. Filapekb, E. Schab-Balcerzak, *Synth. Met.,* 2014, 195, 341-349.

[24] L.N. Ma, H.J. Niu, Cai JW, Y.F. Lian, C.H. Zhang, C. Wang, X.D. Bai, W. Wang, *Sensor. Actuat. B: Chem.,* 2013, 188, 117-126.

[25] H.J. Niu, J.W. Cai, P. Zhao, C. Wang, X.D. Bai, W. Wang, *Dyes. Pigments*., 2013, 96, 158-169.

[26] K. Yamamoto, K. Takanashi, *Polymer,* 2008, 49, 4033-4441.

[27] G. Meshulam, G. Berkovic, Z. Kotler, A. Ben-Asuly, R. Mazor, L. Shapiro, V. Khodorkovsky, *Synth. Met.,* 2000, 115, 219-223.

[28] A. Sakalyte, J. Simokaitiene, A. Tomkeviciene, J. Keruckas, G. Buika, J.V. Grazulevicius, V. Jankauskas, C.P. Hsu, C.H. Yang, *J. Phys. Chem. C,* 2011, 115, 4856-4862.

[29] M.H. Tsai, Y.H. Hong, C.H. Chang, H.C. Su, C.C. Wu, A. Matoliukstyte, J. Simokaitiene, S. Grigalevicius, J. V. Grazulevicius, C. P. Hsu, *Adv. Mater.,* 2007, 19, 862-866.

[30] Y. Olivier, V. Lemaur, J.L. Bredas, J. Cornil, *J. Phys. Chem. A,* 2006, 110, 6356-6364.

[31] O.D. Is, F.B. Koyuncu, S. Koyuncu, E. Ozdemir, *Polymer,* 2010, 51, 1663-1669.

[32] M. Grigoras, N.C. Antonoaia, *Eur. Polym. J.,* 2005, 41, 1079-1089.

[33] T. Abidin, Q. Zhang, K.L. Wang, D.J. Liaw, *Polymer*, 2014, 55, 5293-5304.

[34] (a) M. Palewicz, A. Iwan, J. Doskocz, W. Strek, D. Sek, B. Kaczmarczyk, B. Mazurek, *Polym. Bull.,* 2011, 66, 65–76; (b) D. Sek, E. Grabiec, H. Janeczek, B. Jarzabek, B. Kaczmarczyk, M. Domanski, A. Iwan, *Opt. Mater.,* 2010, 32, 1514-1525.

[35] A. Iwan, D. Sek, *Progr. Polym. Sci.,* 2008, 33, 289-345.

[36] J.C. Hindson, B. Ulgut, R.H. Friend, N.C. Greenham, B. Norder, A. Kotlewskic, T.J. Dingemans, *J. Mater. Chem.,* 2010, 20, 937-944.

[37] W.B. Zhang, C. Wang, G. Liu, J. Wang, Y. Chen, R.W. Li, *Chem. Comm.,* 2014, 50, 11496-11499.

[38] (a) T. Ganicz, W.A. Stanczyk, E. Białecka-F, I. Sledzinska, *Polymer.* 1999, 40, 4733-4739; (b) X.D. Zhuang, Y. Chen, B.X. Li, D.G. Ma, B. Zhang, Y.X. Li, *Chem. Mater.,* 2010, 22, 4455-4461

[39] (a) W.W. Li, C. Gao, H.F. Qian, J.C. Ren, D.Y. Yan, *J. Mater. Chem.,* 2006, 16, 1852-1859; (b) T. Kuorosawa, C.C. Chueh, C.L. Liu, T. Higashihara, M. Ueda, W.C. Chen, *Macromolecules,* 2010, 43, 1236-1244.

[40] (a) J.W. Cai, H.J. Niu, C. Wang, L.N. Ma, X.D. Bai, W. Wang, *Electrochim. Acta.,* 2012, 76, 229-241; (b) H.J. Niu, H.Q. Kang, J.W. Cai, C. Wang, X.D. Bai, W. Wang, *Polym. Chem.,* 2011, 2, 2804-2817.(c) H.J. Niu, P.H. Luo, M.L. Zhang, L. Zhang, L.N. Hao, J. Luo, X.D. Bai, W. Wang, *Eur. Polym. J.,* 2009, 45, 3058-3071.

[41] G.S. Liou, S.H. Hsiao, *J. Polym. Sci. A. Polym. Chem.,* 2003, 41, 94-105.

[42] K. Junji, O. Yoshinori, Japanese Kokai Tokkyo Koho JP2008201676A 20080904 (2008) 50pp.

[43] T. Su, S.H. Hsiao, G.S. Liou, *J. Polym. Sci., Part A: Polym. Chem.,* 2005, 43, 2085–2098.

[44] C. Mallet, M.L. Borgne, M. Starck, W.G. Skene, *Polym. Chem.,* 2013, 4, 250–254.

[45] (a) C.J. Yang, S.A. Jenekhe, *Macromolecules.* 1995, 28, 1180-1196. (b) C.J. Yang, S.A. Jenekhe, *Chem. Mater.,* 1991, 3, 878-887.

[46] (a) A. Iwan, B. Kaczmarczyk, B. Jarzabek, J. Jurusik, M. Domanski, M. Michalak, *J. Polym. Sci., Part A: Polym. Chem.,* 2008, 112, 7556-7566; (b) J. Gąsiorowski, E.D. Głowacki, B. Hajduk, M. Siwy, M.C. Ogierman, J. Weszka, H. Neugebauer, N.S. Sariciftci, *J. Phys. Chem. C,* 2013, 117, 2584−2589.

[47] S.A. Jenekhe, L. Lu, M.M. Alam, *Macromolecules,* 2001, 34, 7315-7324.

[48] H.M. Wang, S.H. Hsiao, G.S. Liou, C.H. Sun, *J. Polym. Sci. A. Polym. Chem.,* 2010, 48, 4775–4789.

[49] Wang, J., Analytical Electrochemistry, Third Edn., New Jersey: WILEY-VCH, 2006, 169.

[50] H.J. Yen, S.M. Guo, G.S. Liou, J.C. Chung, Y.C. Liu, Y.F. Lu, Y.Z. Zeng, *J. Polym. Sci., Part A: Polym. Chem.,* 2011, 49, 3805–3816.

[51] M.J. Frisch, G.W. Trucks, H.B. Schlegel, G.E. Scuseria, M.A. Robb, J.R. Cheeseman,V.G. Zakrzewski, J.A. Montgomery Jr., R.E. Stratmann, J.C. Burant, S. Dapprich,J.M. Millam, A.D. Daniels, K.N. Kudin, M.C. Strain, O. Farkas, J. Tomasi, V. Barone,M. Cossi, R. Cammi, B. Mennucci, C. Pomelli, C. Adamo, S. Clifford, J. Ochterski,G.A. Petersson, P.Y. Ayala, Q. Cui, K. Morokuma, D.K. Malick, A.D. Rabuck, K.Raghavachari, J.B. Foresman, J. Cioslowski, J.V. Ortiz, A.G. Baboul, B.B. Stefanov,G. Liu, A. Liashenko, P. Piskorz, I. Komaromi, R. Gomperts, R.L. Martin, D.J. Fox,T. Keith, M.A. Al-Laham, C.Y. Peng, A. Nanayakkara, M. Challacombe, P.M.W.Gill, B. Johnson, W. Chen, M.W. Wong, J.L.

Andres, C. Gonzalez, M. HeadGordon, E.S. Replogle, J.A. Pople, GAUSSIAN 98, Gaussian, Inc., Pittsburgh, PA,1998.

Captions

Scheme.1. Synthetic routes for PAM 1-6 with different diamines.

Fig.1. TGA curves of PAM1 to PAM6.

Table 1 Thermal properties and molecular weights of the PAMs.

Fig.2. UV-visible absorption spectra (A) and PL spectra (B) of PAMs in CH_2Cl_2 at room temperature, (C) the CIE 1931 (x, y) chromaticity diagram of PAMs.

Table 2. Optical and electrochemical properties for PAMs.

Fig.3. Absorbance spectral changes of PAM3 and PAM6 in CH_2Cl_2 when protonated with HCl vapor in steps during the same time interval. The concentration of pure PAMs was 0.034 mg/L. Inset: photographs showing the color changes upon HCl vapor exposure. The undoped molecular structure and protonated extreme resonance forms of PAMs shown on right.

Fig.4. Photograph of the PL of PAM3 and PAM6 in the ailica gel plate upon UV exposure (excited at 365 nm).

Fig.5. Cyclic voltammetry for PAMs in CH_3CN containing 0.1mol/L $LiClO_4$, at a scan rate of 50 mV/s.

Scheme.2. Proposed simplified redox process and the resonance form of PAM2, PAM3 and PAM5.

Fig.6. Pictorial representations (a) of the electron density in the frontier molecular-orbitals of repetition units and pictorial energy gap (b) of PAMs.

Fig.7. Electronic absorption spectra of films of PAM2 (a) and PAM5 (b) and their 3D spectra respectively, in the process of electrochemical doping with 0.1 V potential intervals in CH_3CN containing 0.1mol/L $LiClO_4$ as the supporting electrolyte (vs Ag/AgCl).

Fig.8.(a) Potential step absorptiometry (upper) and (b) current consumption (lower) of PAM5 at 505 nm (in 0.1 mol/L $LiClO_4/CH_3CN$ as the supporting electrolyte) by applying a potential step (0.00-0.80 V) with a cycle time of 10 s.

Table 3. Optical and electrochemical date collected for coloration efficiency measurements of PAMs.

Fig.9. A typical photocurrent (lower) and photovoltaic (upper) response for an PAM6 film immobilized on ITO glass upon exposure to light with switching at room temperature. (b) photogenerated electrons flow scheme.

Fig 1

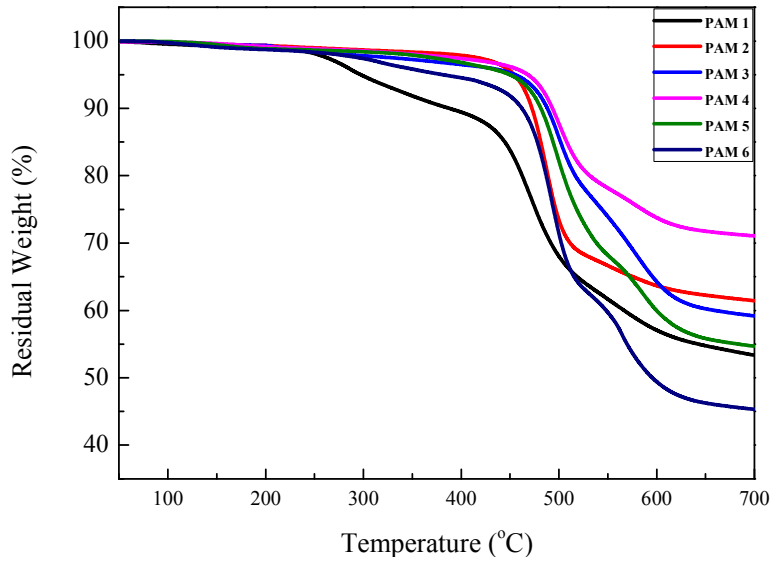

Fig.1. TGA curves of PAM1 to PAM6.

Fig 2

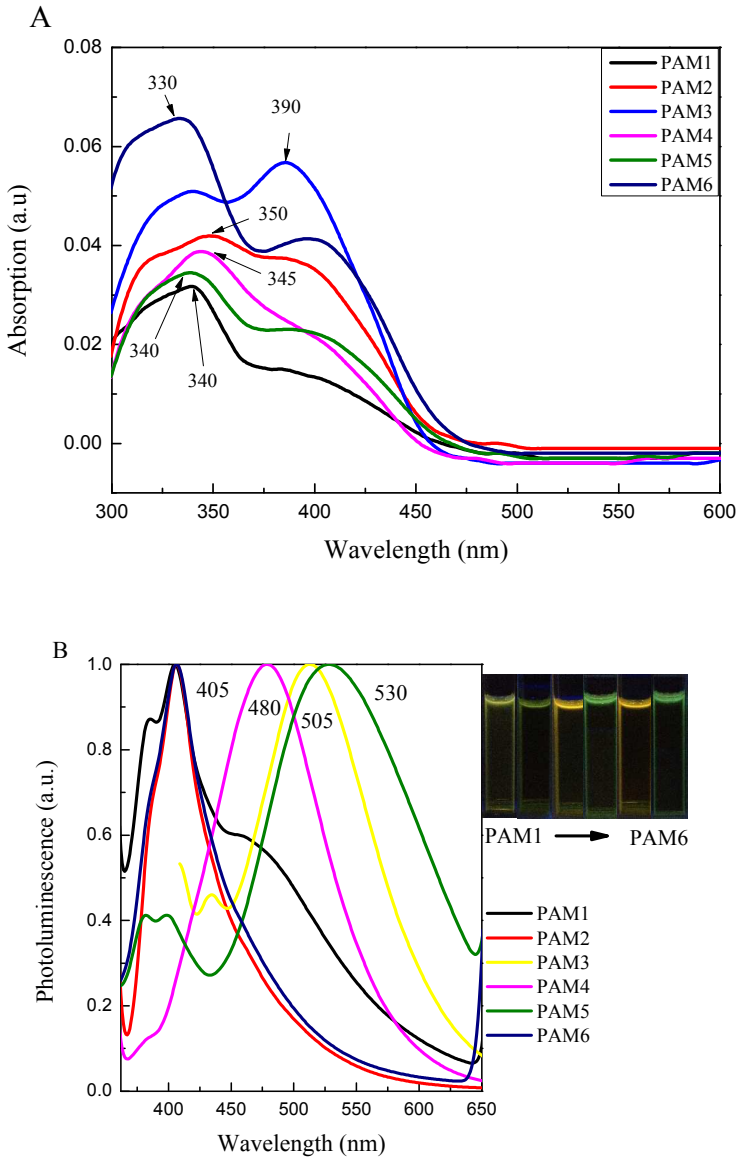

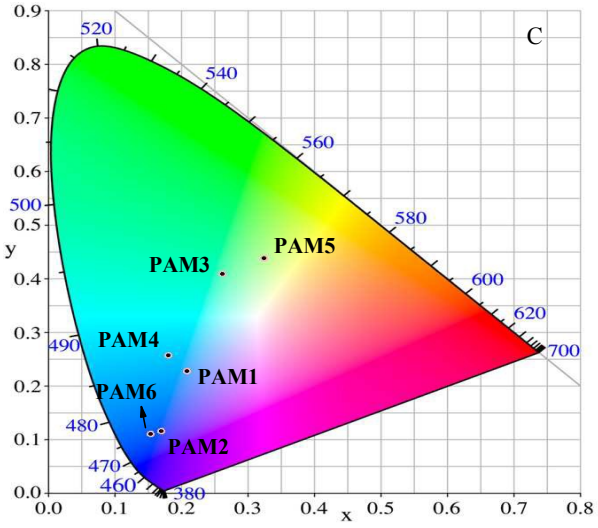

Fig.2. UV-visible absorption spectra (A) and PL spectra (B) of PAMs in CH_2Cl_2 at room temperature, (C) the CIE 1931 (x,y) chromaticity diagram of PAMs.

Fig 3

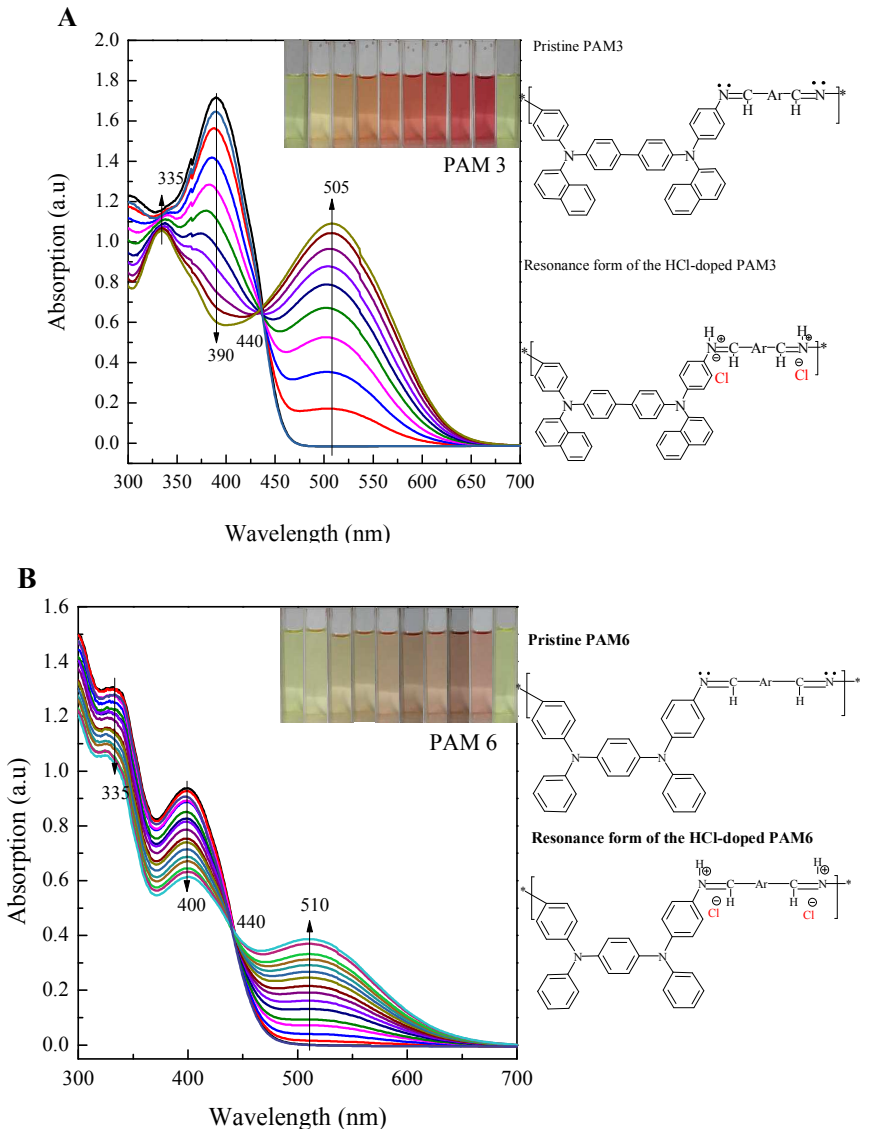

Fig.3. Absorbance spectral changes of PAM3 and PAM6 in CH_2Cl_2 when protonated with HCl vapor in steps during the same time interval. The concentration of pure PAMs was 0.034 mg/L. Inset: photographs showing the color changes upon HCl vapor exposure. The undoped molecular structure and protonated extreme resonance forms of PAMs shown on right.

Fig 4

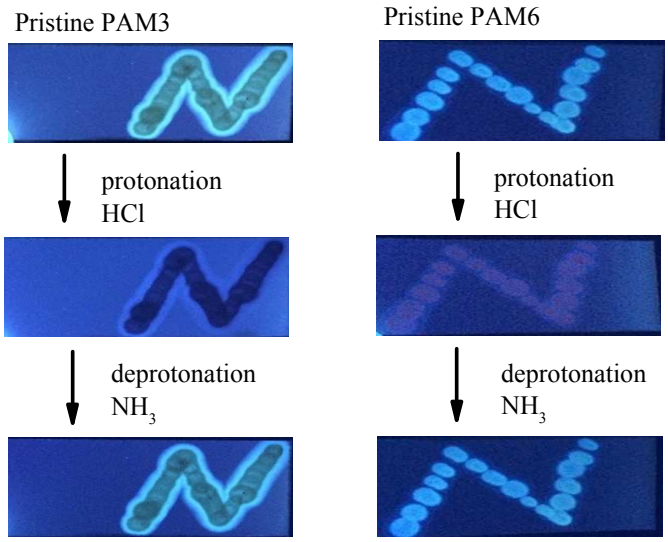

Fig.4. Photograph of the PL of PAM3 and PAM6 in the silica gel plate upon UV exposure (excited at 365 nm).

Fig 5

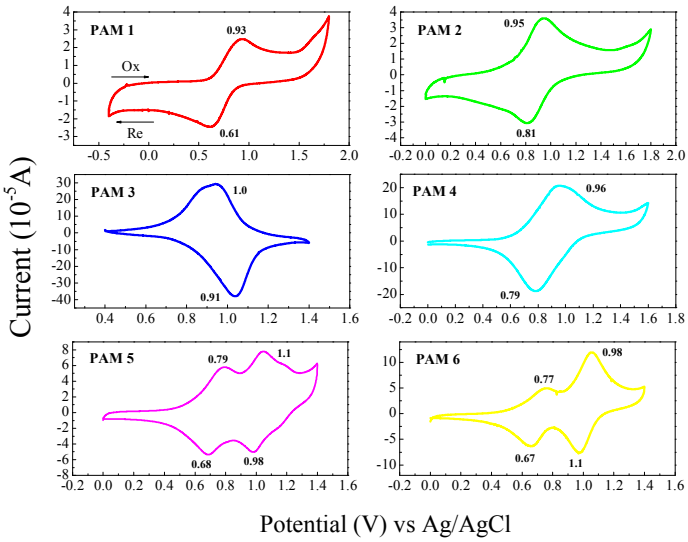

Fig.5. Cyclic voltammtry for PAMs in CH_3CN containing 0.1mol/L $LiClO_4$, at a scan rate of 50 mV/s.

Fig 6

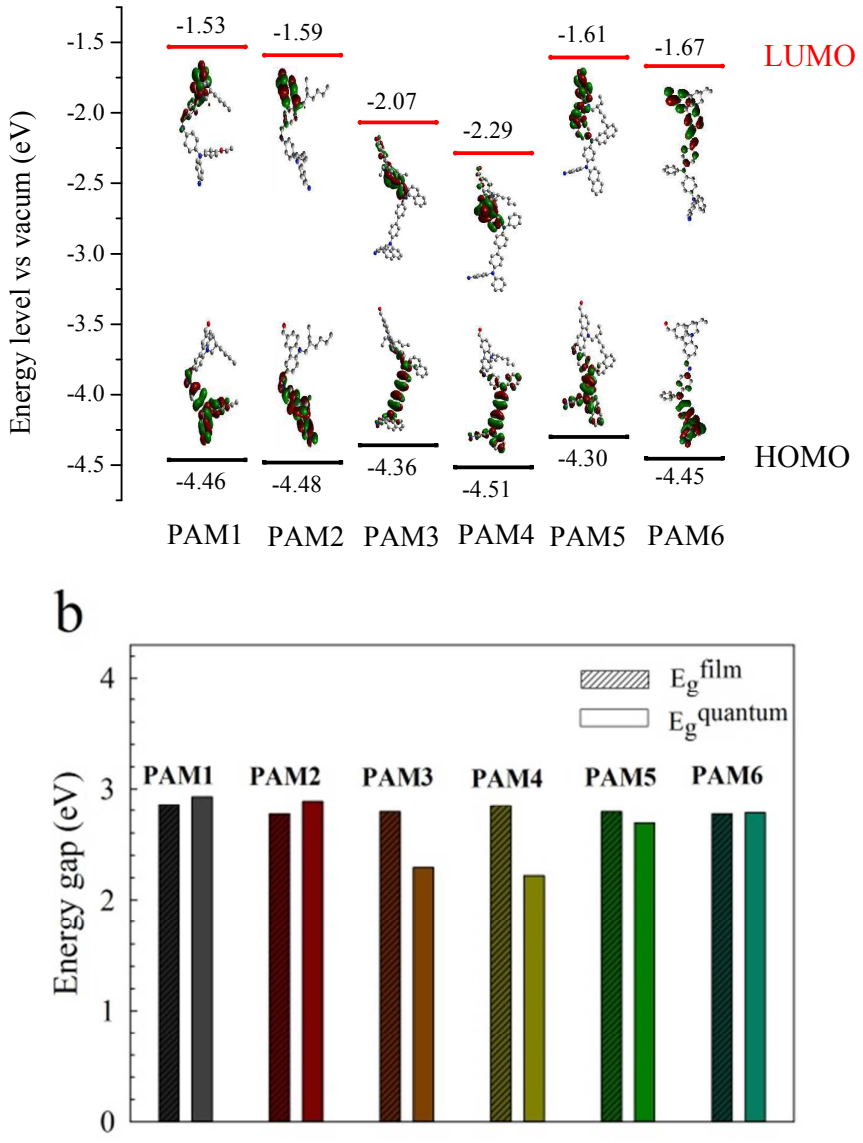

Fig.6. Pictorial representations (a) of the electron density in the frontier molecular-orbitals of repetition units and pictorial energy gap (b) of PAMs.

Fig 7

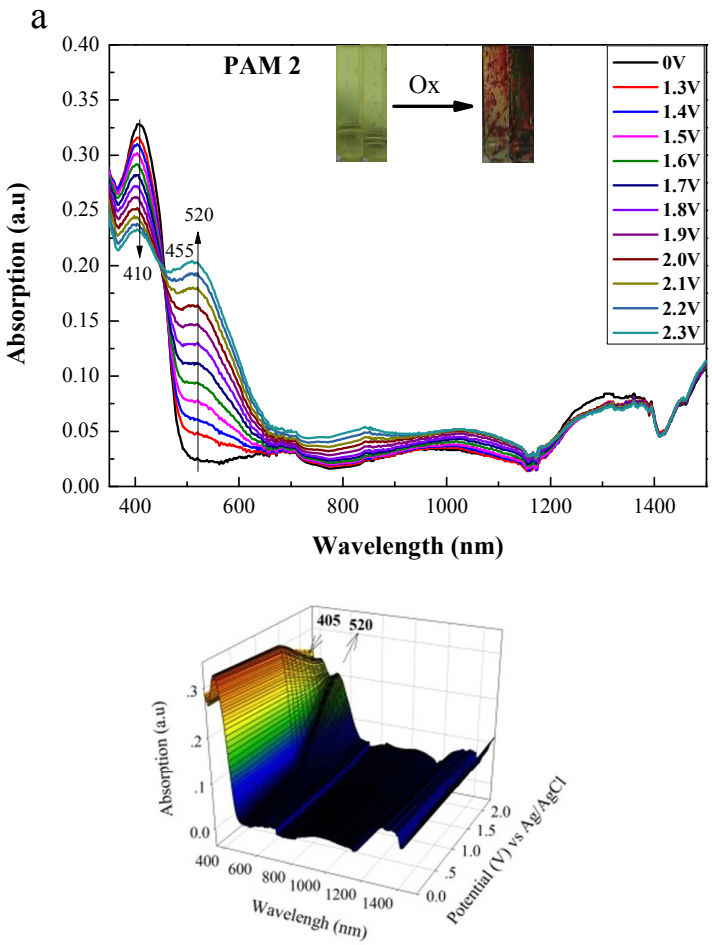

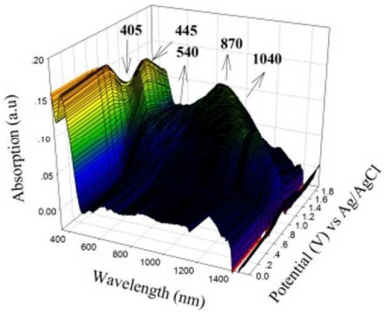

Fig.7. Electronic absorption spectra of films of PAM2 (a) and PAM5 (b) and their 3D spectra respectively, in the process of electrochemical doping with 0.1 V potential intervals in CH_3CN containing 0.1mol/L $LiClO_4$ as the supporting electrolyte (vs Ag/AgCl).

Fig 8

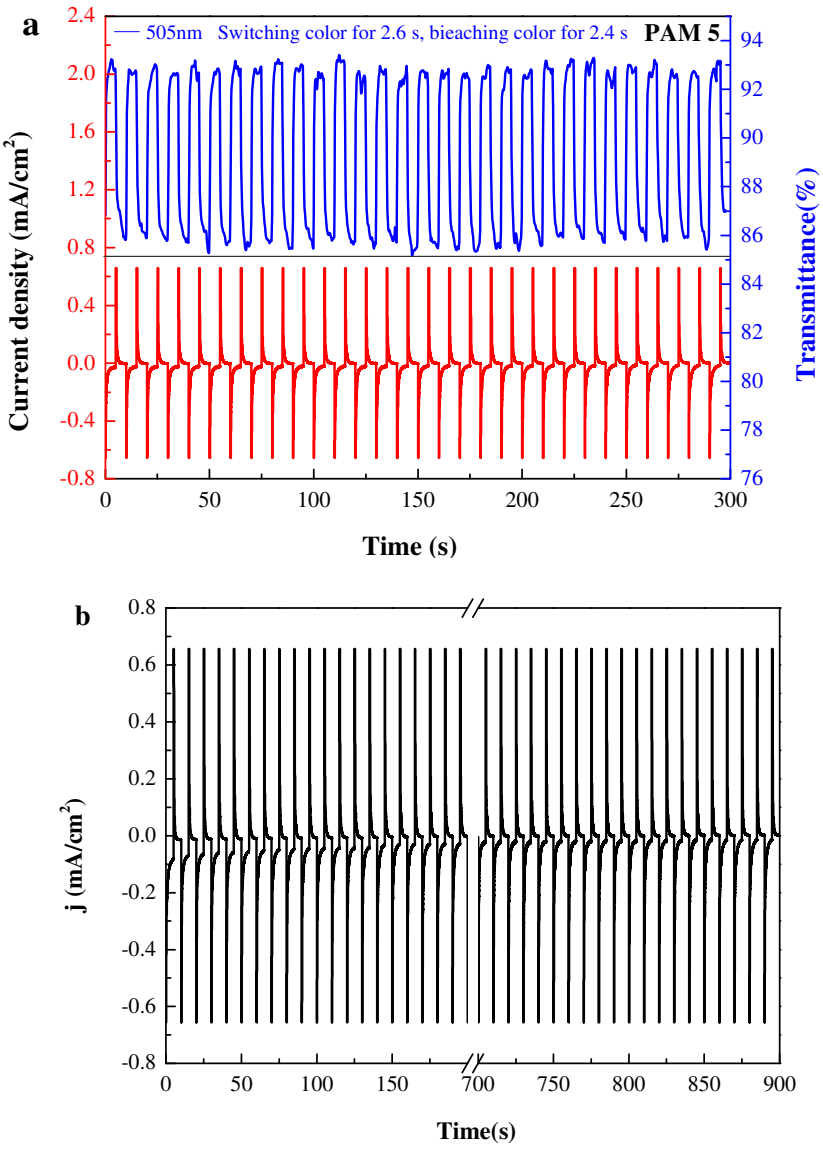

Fig.8.(a) Potential step absorptometry (upper) and (b) current consumption (lower) of PAM5 at 505 nm (in 0.1 mol/L $LiClO_4/CH_3CN$ as the supporting electrolyte) by applying a potential step (0.00-0.80 V) with a cycle time of 10 s.

Fig 9

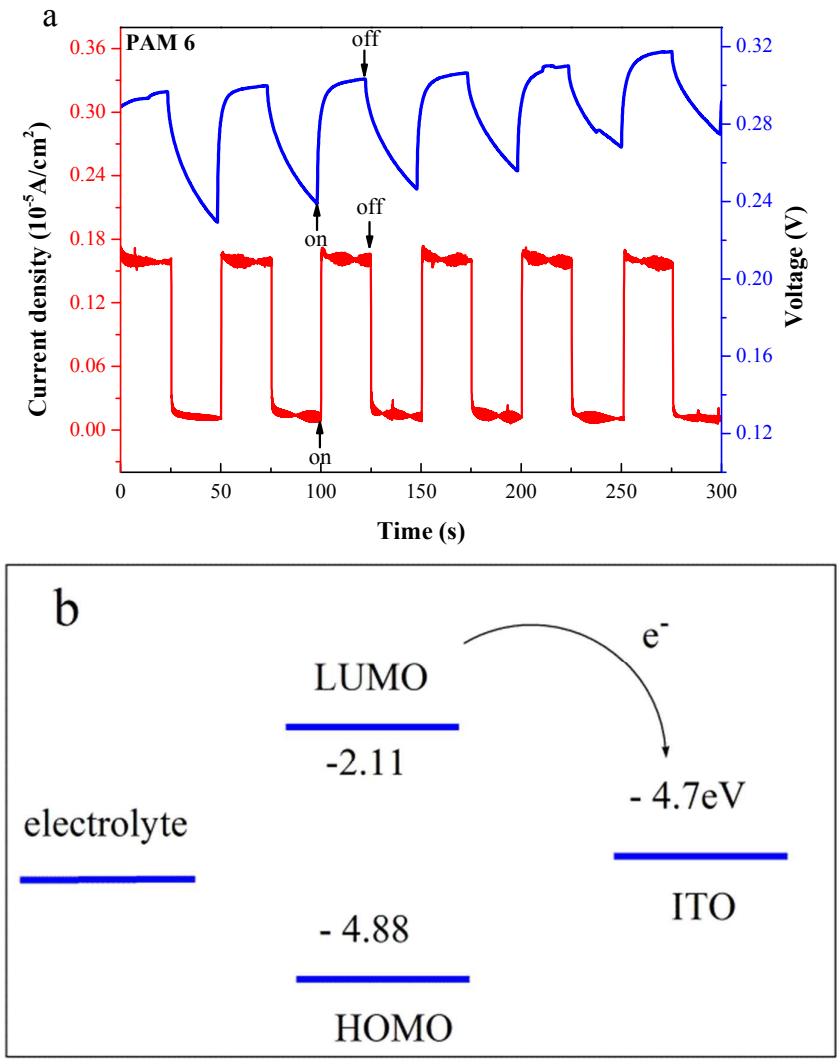

Fig.9. A typical photocurrent (lower) and photovoltaic (upper) response for an PAM6 film immobilized on ITO glass upon exposure to light with switching at room temperature. (b) photogenerated electrons flow scheme.